Spectral Characterization of a Blue-Enhanced Silicon Photodetector

Michael L. F. Lerch, *Member, IEEE*, Anatoly B. Rosenfeld, *Senior Member, IEEE*, Phillip E. Simmonds, Geoffery N. Taylor, Steve R. Meikle, *Member, IEEE*, and Vladimir L. Perevertailo

Abstract—In this paper, we report on spectral response data and gamma ray spectroscopy measurements using two newly developed silicon photodetectors that are designed to have enhanced sensitivity in the blue spectral region. The enhanced sensitivity is a result of our newly developed ion implantation profile used to create the active area of the photodetector. The quantum efficiency of the new photodetectors (without any optimized antireflective coating) has been measured to be ~40% at a wavelength of 420 nm. Gamma ray spectroscopy experiments have been performed using a thallium doped cesium iodide, [CsI(Tl)], and a cerium doped lutetium oxy-orthosilicate, (LSO) crystal excited by a ^{137}Cs or ^{22}Na source and read out by the new photodetectors. We have measured an energy resolution of 7.7% and 22.7% full-width at half-maximum (FWHM) for the 662-keV gamma rays from a ^{137}Cs for the CsI(Tl) and LSO scintillator crystal respectively. We intend to use the photodetectors, in the form of a detector array optically coupled to CsI(Tl) or LSO, in the development of a new scintillator detector module for use in positron emission tomography (PET).

Index Terms—Detector module, positron emission tomography (PET), silicon photodetector.

I. INTRODUCTION

THE ultimate aim of this research is to produce a new detector module suitable for use in positron emission tomography (PET). The design of the detector module will not include photomultiplier tubes, instead an array of silicon photodiodes (PDs) will be used to readout the scintillation crystals. In this case, the necessary timing and energy signal must be generated solely from the PDs. The present article centers on the development of PDs that have characteristics to match such needs of PET detectors [1]. We use a special ion implantation technique to create the active region optically coupled to the scintillator crystals. The technique gives rise to enhanced sensitivity in the blue spectral region, where many common scintillation crystal emission spectra extend into [e.g., CsI(Tl)] or peak (e.g., LSO), while still maintaining good charge collection properties, ensuring a fast rise time of the detector signal for timing purposes.

In designing the new detector module, we have performed extensive Monte Carlo simulations based on using the new PD as part of an 8 × 8 silicon pixel array coupled to a 25 × 25 × 3 mm^3 LSO or CsI(Tl) scintillator crystal. The simulations predicted that for any position of a gamma ray interaction in the scintillator crystal, the spatial resolution and signal-to-noise ratio (SNR) obtained by the new detector arrangement would be satisfactory in order to obtain the gamma ray interaction position in the plane of the silicon photodetector.

The detector arrangement can then be configured to form a PET detector module with total dimensions 4 × 25 × 80 mm^3, which includes associated readout electronics. In our module the pixel photodetectors (with an effective active area of 25 × 25 mm^2) are placed on the side of the scintillator crystal with matched surface dimensions. More details on the PET module design will be discussed elsewhere.

The new detectors, designed by the Center for Medical Radiation Physics at the University of Wollongong in collaboration with the High Energy Physics Department, University of Melbourne, were produced by SPA "Detector," Ukraine. This work concentrates on the spectral performance of the new photodetector using optical excitation spectroscopy and gamma ray spectroscopy.

II. METHODS

A. Spectral Response

The spectral response of the photodetectors was determined by using standard modulation techniques. The light from a quartz-halogen lamp, operated at a constant current, was chopped and focused on the entrance slit of a 1-m spectrometer (SPEX model 1704). The light exiting the spectrometer passed through a 1-mm iris before being incident on the photodetector. The photodetectors were positioned accurately at a constant distance from the iris and the incident beam was carefully centered on the photodetector. The lamp power was monitored and fluctuations in the lamp power of order 1% could be observed in the response of the photodetectors. The linearity and modulation frequency independence of the measured response was checked.

Under the same experimental conditions the spectral response of a Hamamatsu (model S3590-08) photodiode was measured. Using this data and the specification data sheets provided by Hamamatsu, the absolute responsivity and corresponding quantum efficiency of the photodiodes could then be deduced. Details are given in Section IV-B.

B. Gamma Ray Spectroscopy

Room temperature spectroscopy experiments were performed on the isolated photodetector elements. The photodetectors were optically coupled to a $4 \times 4 \times 10$ mm^3 LSO (purchased from CTI) or a $3 \times 3 \times 3$ mm^3 CsI(Tl) crystal (purchased from AMCRYS-H) using BICRON optical grease. All LSO crystal surfaces were polished. All of the CsI(Tl) crystal surfaces were smooth but not polished. Crystal surfaces not in contact with the photodetector were covered with several layers of Teflon tape.

The scintillators were excited via a ^{137}Cs or ^{22}Na source. The spectroscopy readout arrangement comprised of an ORTEC 142A preamplifier and an ORTEC 671, spectroscopy amplifier. A PC, using software supplied with the MCA, collected data via an AMPTEK 8000A MCA.

III. NEW DETECTOR DESIGN

The ultimate aim of the present work is to develop a detector module for use in positron emission tomography, which is completely independent of photomultiplier tubes. The new detector module will utilize 8×8 arrays of silicon photodiodes (each with a 3×3 mm^2 active area) to readout the scintillator crystal of interest. We have chosen silicon photodiodes as they are very robust and relatively cheap to manufacture. The main drawback in using photodiodes is that there is no internal amplification process involved in the conversion of the optical signal to an electrical signal. In this case careful design considerations must be taken into account to ensure a satisfactory final signal to noise ratio.

We intend to use LSO or CsI(Tl) scintillator crystals in our module that have emission spectra which peak at 420 nm and 540 nm, respectively. The absorption length of light with a wavelength of 420 nm is 0.1–0.2 μm [2]. In order to improve the sensitivity of the new photodiodes at wavelengths in the region of 400nm we are using a special (boron) ion implantation technique [3] to produce the p$^-$-layer that is optically coupled to the scintillator crystal. The resulting p$^-$-layer (schematically shown in Fig. 1) extends to a depth of 0.6 μm with the peak in the carrier concentration occurring at 0.14 μm. The new technique allows the resulting electric field to extend very close to the p$^-$ active surface, which has the dimensions of 3×3 mm^2 for each pixel element in our array, when the PD is under bias while still maintaining the potential across the p$^-$ surface. In effect we are able to improve the sensitivity of the PD in the blue spectral region, by reducing the effect of Auger recombination, while maintaining good charge collection properties to ensure fast timing signals for coincident detection techniques. We have optimized the trade-off between good spectral sensitivity (near 420 nm) and fast charge collection of the photodetectors by performing charge collection modeling of the new ion implantation profile using Integrated Systems Engineering (ISE) TCAD simulation software including (DESSIS, LIGAMENT, PROSIT, TE2DIOS)," Release 4.0 ed. Zurich.

Using this technique, we have produced two new silicon photodiodes which should have an improved sensitivity in the blue spectral region as a result of the enhanced electric field at the
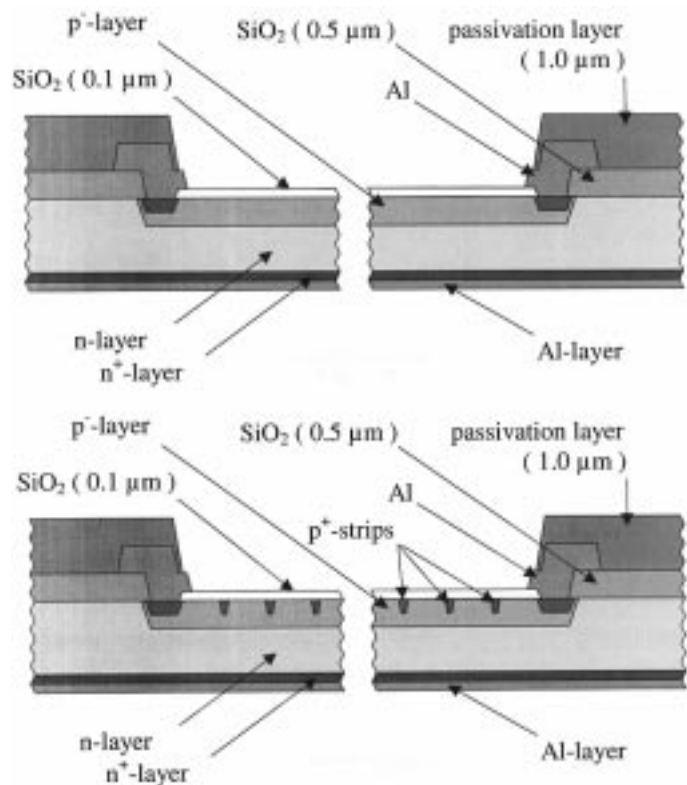

Fig. 1. Schematic diagram of the two detector designs under investigation. The main difference in the two designs is the introduction of a series of p$^+$ strips [as indicated in Fig. 1(bottom)] in the uniform p$^-$ layer which makes up the active region of the detectors. (top) SPAD1 and (bottom) SPAD2.

surface of the PD. Schematic views of the two new detector designs are shown in Fig. 1. The two designs differ in that one has a uniform p$^-$ layer at the surface and the other has p$^+$ strips, with 300 μm separation, embedded in the p$^-$ layer. They are here-on in referred to as SPAD1 and SPAD2 respectively.

The two approaches in detector design were undertaken to investigate the effect of the p$^+$ strips in the uniform p$^-$ layer on both the spectral response of the PD, especially in the region of 400 nm, and the timing properties of the PDs.

It should be noted that it is fairly common practice in the design of modern photodetectors to incorporate an optically transparent antireflective coating (ARC) that covers the active layer of the photodetector [2], in our case the p$^-$ layer. The ARC acts as a quarter-wave plate to minimize reflections from the detector surface at a particular wavelength of interest, effectively improving the quantum efficiency of the PD. The wavelength of interest is determined by the thickness and the refractive index of the ARC. For our detectors we have deliberately chosen not to use an ARC thickness that would improve the measured quantum efficiency around 400 nm in an attempt to isolate the blue spectral sensitivity enhancement of the detector that results from our ion implantation technique.

The results from experiments described within this paper arise from 5×5 mm^2 photodetectors individually mounted, but manufactured from the same wafer as the detector arrays. The photodiodes are of a planar design consisting of a 3×3 mm^2 active area and are 300 μm thick. The active area is surrounded by a p$^+$ guard ring and all encircled by an n$^+$
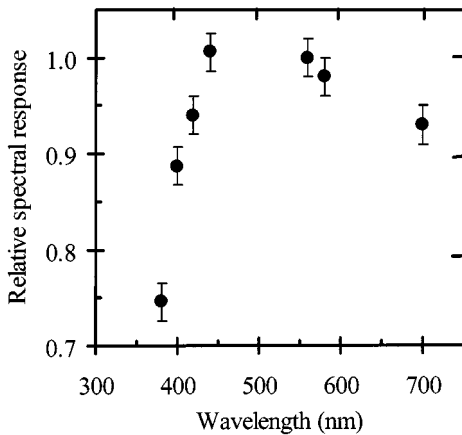
Fig. 2. Spectral response of SPAD2 relative to SPAD1. The significant loss in spectral response measured at 380 nm is due to the p$^+$ layers embedded into the shallow p$^-$-layer that forms the active area of the photodiode.

Fig. 3. Spectral response of SPAD1 relative to the Hamamatsu S3590-08, blue enhanced, photodiode.

ring. The detectors were produced by SPA "Detector" on high resistivity n-Si (Waker, resistivity 5 kΩ·cm). The SPAD1 and SPAD2 photodetectors are operated at 40 V and have a room temperature dark current and capacitance of $\sim$1.4 nAcm^{-2} and 5.7 pF at this voltage. The noise of the detection system under standard operating conditions is equivalent to 250 electrons.

IV. RESULTS

A. Spectral Response

The ratio of the absolute spectral response between 380 nm and 700 nm for the two new photodetectors is shown in Fig. 2. The loss in spectral response due to the introduction of the p$^+$ strips in SPAD2 is evident in the relative response for wavelengths below 440 nm. Above 440 nm the effect of the p$^+$ strips is expected to be much less significant as the light on average travels further into the detector before being detected and the p$^+$ stirps are at a very shallow implantation depth. For $\lambda = 380$ nm there is a loss in spectral response of approximately 30% which corresponds to the effective loss in active area due to the finite width (in the plane of the detector surface) of the p$^+$ strips. For wavelengths around 700 nm the slight loss in spectral response is possibly due a slight difference in thickness of the silicon dioxide coating between the two detectors.

Fig. 3 shows the spectral response of SPAD1 relative to the Hamamatsu S3590-08 over the wavelength range of 380 nm to 700 nm. The spectral response of the SPAD1 PD is less than that of the Hamamatu PD over most of the measured wavelength range. At 700 nm the spectral response of the SPAD1 PD is slightly greater than that of the Hamamatsu PD. The above results are attributed to the silicon dioxide layer acting as an antireflective coating for longer wavelengths in the case of the SPAD1 PD design. The current version of the photodetector was produced with a coating of silicon dioxide of thickness approximately 0.1 μm (in the plane perpendicular to the detector surface), which is not optimized for the blue spectral region. The Hamamatsu S3590-08 is optimized for detection of light in the blue spectral region and may account for the observed difference. Such optimization has been shown to have a significant long wavelength tail [2].
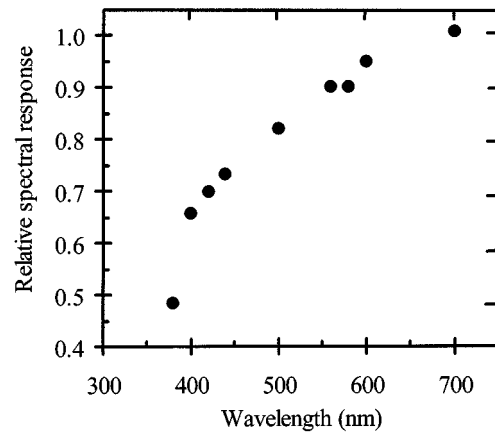
In Fig. 3, there is only a small measured effect of the ARC used in conjunction with SPAD1 in the wavelength region near 700 nm. The effect of the ARC for the SPAD1 PD will only be observed in the relative spectral response data near the peak of the SPAD1 PD spectral enhancement. Such a result is due to the increased absorption length (in the photodetector) of light with increasing wavelength combined with the tailing nature of the blue enhancement of the S3590-08 PD mentioned above.

B. Quantum Efficiency

The quantum efficiency, Q_e, of the SPAD1 photodetector was deduced using the Hamamatsu photodiode as a reference. The relative responsivity curve of the S3590-08 photodiode was measured and corrected for the lamp output power dependence on the wavelength, (which was independently determined using a photomultiplier tube). The corrected curve was in good agreement with the shape of the absolute responsivity, R, curve in the data sheets supplied by Hamamatsu. The quantum efficiency of the S3590-08 was then derived using the relationship

$$Q_e = R \times h\nu \tag{1}$$

where R is the absolute responsivity in A/W of the S3590-08, and $h\nu$ is the energy of the photoelectrons in eV.

Fig. 4 shows the quantum efficiency of the SPAD1 photodiode over the wavelength range of 380 nm to 700 nm. The deduced quantum efficiency at 420 nm is $\sim$40%. Holland et al. [2] used a different approach to design a photodiode array for PET by reducing the polysilicon layer associated with the n$^+$ contact layer to improve the quantum efficiency near 420 nm. In our diode, we produce the n$^+$ rear contact via the classical ion implanted detector method using evaporated aluminum to produce the uniform potential across the rear surface of the 25 $\times$ 25 mm^2 array. Our deduced quantum efficiency indicates that the SPAD1 PD is equivalent to a backside illuminated PD as produced by Holland et al. with a 20 nm polysilicon layer without any antireflective coating. According to the same work [2], the quantum efficiency will increase by a factor of $\sim$1.7 when we incorporate an antireflective coating optimized for the collection of 420 nm light. In this case the quantum efficiency will increase to nearly 70%.
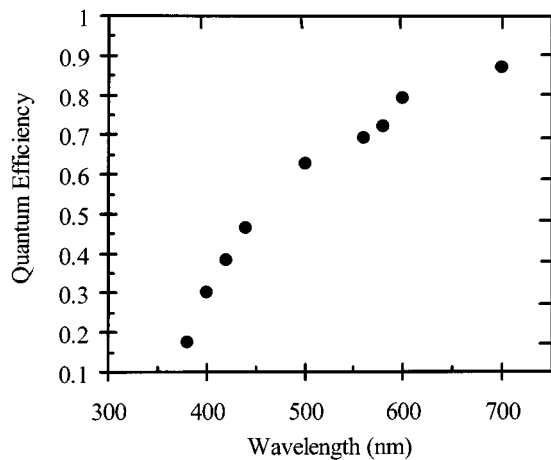
Fig. 4.   Deduced quantum efficiency as a function of wavelength for the new photodiode, SPAD1.
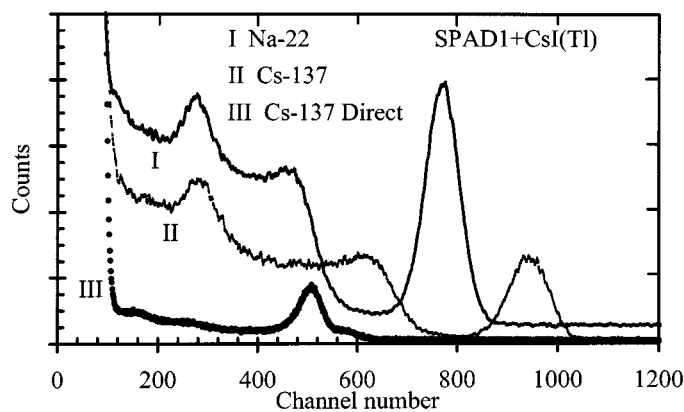

Fig. 6.   Room temperature, pulse height spectrum of a LSO crystal excited by I ^{22}Na and II ^{137}Cs. The LSO crystal was read out by the SPAD1 PD. Spectrum III is the 32 and 36 keV X-ray spectrum of ^{137}Cs directly detected by the PD and is scaled by a factor of ten beyond channel number 275 for clarity.

Fig. 5.   Room temperature, pulse height spectrum of a 3 × 3 × 3 mm^3 CsI(Tl) crystal excited by I ^{22}Na and II ^{137}Cs read out by the SPAD1 PD. Spectrum III is the 32 and 36 keV X-ray spectrum of ^{137}Cs directly detected by the PD.

C. Gamma Ray Spectroscopy

The SPAD1 PD was optically coupled, in separate experiments, to a 3 × 3 × 3 mm^3 CsI(Tl) scintillator crystal and a 4 × 4 × 10 mm^3 LSO crystal. The results are shown in Figs. 5 and 6, respectively.

Fig. 5 shows the room temperature (298 K) pulse height spectrum resulting from a CsI(Tl) crystal excited by a ^{22}Na (spectrum I) and ^{137}Cs (spectrum II) source as measured by the SPAD1 PD. In these experiments a 3 -μs shaping time was used. Overlayed is the X-ray spectrum from a ^{137}Cs source (spectrum III) measured directly by the photodetector. The X-ray spectrum serves as a convenient benchmark for a calculation of the light collection efficiency. The observed feature in spectrum III results from the detection of the 32 and 36 keV X-ray emission (just unresolved).

Fig. 6 shows the corresponding pulse height spectrum from a 4 × 4 × 10 mm^3 LSO crystal excited by a ^{22}Na (spectrum I) and ^{137}Cs (spectrum II) source and read out by the SPAD1 PD. In these experiments a 1 μs shaping time was used. Again the X-ray spectrum from a ^{137}Cs source (spectrum III) is overlayed. Spectra III in Fig. 6 has been scaled by a factor of ten above channel 275 for clarity.
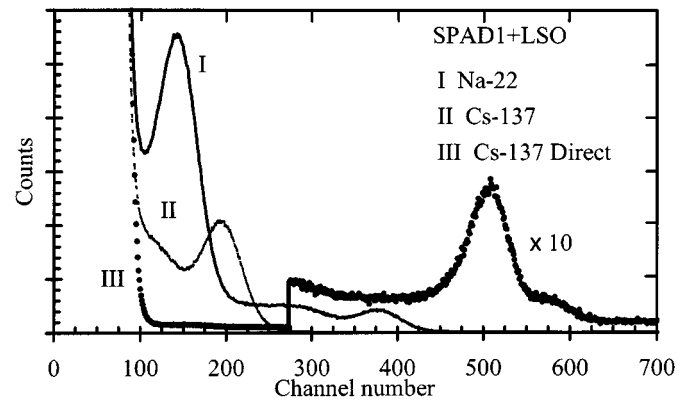
1) Energy Resolution: Using the 3 × 3 × 3 mm^3 CsI(Tl) crystal optically coupled to the SPAD1 PD we measured an energy resolution of 7.7% fullwidth at half maximum (FWHM) when excited with 662-keV gamma rays from a ^{137}Cs source and 9.5% FWHM when excited with 511 keV gamma rays from a ^{22}Na source. These values compare very well with some of the best values quoted in the literature for silicon photodiodes. Varying the spectroscopy amplifier shaping time between 1 and 3 μs had no significant effect on the measured energy resolution. Operation outside these shaping times saw a measured degradation of the energy resolution.

The 4 × 4 × 10 mm^3 LSO crystal read out by the SPAD1 PD, had a measured energy resolution of 22.7% FWHM when excited with 662 keV gamma rays from a ^{137}Cs source. Excitation using the 511 keV and the 1275-keV gamma rays from a ^{22}Na source led to a measured energy resolution of 28.8% and 16% FWHM, respectively. The measured energy resolution results LSO are also within the range of those quoted in the literature for readout schemes of scintillator crystals using silicon PDs.

The measured relative energy resolution for LSO will improve once we incorporate an antireflective coating optimized for wavelengths in region of 420 nm.

2) Light Detection Efficiency: The light detection efficiency refers to the calculated number of photons detected by the PD as a fraction (or percentage) of the absolute number of photons emitted by the scintillator crystal when excited by a photon of given energy.

The general method to maximize the light detection efficiency is to use several layers of Teflon tape. However, various scintillator crystal surface finishes ranging from chemical etching [4] to covering with millepore filter paper [5], for example, can have a significant effect on the overall light collection efficiency. Also, the effect of poor scintillator crystal coupling to detectors has been shown to be significant [5].

An estimate of the light detection efficiency can be easily determined by comparing the ^{137}Cs X-ray photopeak channel with the gamma ray photopeak channel arising from the scintillator crystal under the same experimental conditions. The direct detection of the ^{137}Cs X-rays of energy 34 keV (average of the

32 and 36 keV X-rays) gives rise to the peak at channel 500 in spectrum III in Figs. 5 and 6. We estimate that on average there are ~9400 photoelectrons created within the silicon PD for each 34 keV X-ray interaction.

The absolute light output of LSO has been estimated at 27 000 photons/MeV (13 500 photons per 511 keV) [6]. From spectrum I in Fig. 6 and the X-ray data above we estimate ~4000 photoelectrons are created in the SPAD1 PD for each 511 keV gamma ray interaction in the LSO crystal. The corresponding light detection efficiency is then 30%.

The poor light detection efficiency can be explained by the high light loss due to the difference between active area of the photodetector and the area of the scintillator crystal face. The 4×4 mm^2 LSO crystal face was optically coupled to the photodetector with an active area of 3×3 mm^2. Therefore about 40% of the optical photons exiting the crystal face are not detected by the photodetector.

It is worth noting that in the simple analysis above we have not taken into account any light losses resulting from a meniscus associated with the optical contact. Such factors have been shown to have an impact in determining the measured light output of the photodetector using gamma ray spectroscopy methods [5]. It was shown that even perfect coupling (no meniscus) of a 6×6 mm^2 crystal face to a photodetector with an active area of 6×6 mm^2 led to a reduction in the measured light output of ~20%. The reduction is due to the significance of edge losses at the crystal/photodetector interface, and becomes more significant as the crystal/photodetector area decreases.

V. CONCLUSION

An investigation has been performed into the spectral response of a new photodiode designed to have a good sensitivity in the blue spectral region. The sensitivity without antireflective coating matches the best known published work for similar diodes (but irradiated from the backside) and is a result of a special ion implantation process used to produce an enhanced electric field that extends very close to the detector surface when under reverse bias. The advantage in such a diode design is the shorter hole collection time compared to the backside illuminated detector with the same blue sensitivity. The fast hole collection time will improve the timing properties of the photodetector. Excellent photodetector timing properties are an absolute requirement of PET detector modules that utilize coincident detection techniques.

Two photodiodes were designed and manufactured. The two designs differ in that one (SPAD1) has a uniform p$^-$ layer at the surface and the other (SPAD2) has p$^+$ strips embedded in the p$^-$ layer. The silicon dioxide coating incorporated in both photodetectors was designed not to enhance the spectral response at wavelength less than 600 nm. Such a design allowed us to isolate the spectral enhancement due to the new ion implantation technique. The spectral response data of the two photodetectors showed that they both have an enhanced sensitivity to wavelengths in the blue region. The quantum efficiency of SPAD1 was deduced to be 40% at 420 nm. The response of SPAD2 degraded at short wavelengths ($\lambda < 400$ nm) due to the embedded p$^+$ strips as expected. Further work will need to be done to ensure that the blue enhanced sensitivity does not have a detrimental effect on the timing properties of the new photodiodes.

Gamma ray spectroscopy results using scintillator crystals readout by one of the two new photodiodes indicate that the new photodiode is suitable for use with either LSO or CsI(Tl). The measured energy resolution was 7.7% for a $3 \times 3 \times 3$ mm^3 CsI(Tl) excited by the 662 keV gamma rays from a Cs-137 source. The equivalent for a $4 \times 4 \times 10$ mm^3 LSO scintillator crystal was 22.7%.

We intend to incorporate an antireflective coating, optimized for the detection of light with a wavelength of 420 nm, into the photodiode design. As a result the quantum efficiency will improve to ~70% at 420 nm.

The new photodiodes will be incorporated, in the form of an 8×8 silicon pixel array coupled to a $25 \times 25 \times 3$ mm^3 LSO or CsI(Tl) scintillator crystal, into the design of a new PET detector module.

REFERENCES

[1] S. E. Derenzo, W. W. Moses, R. H. Huesman, and T. F. Budinger, "Critical instrumentation issues for 2 mm resolution, high sensitivity brain PET," in *Quantification of Brain Function*, K. Uemura, N. A. Lassen, and T. Jones, *et al.*, Eds.   Amsterdam, The Netherlands: Elsevier, 1993, pp. 25–37.

[2] S. E. Holland, N. W. Wang, and W. W. Moses, "Development of low noise, back-side illuminated silicon photodiode arrays," *IEEE Trans. Nucl. Sci.*, vol. 44, pp. 443–447, June 1997.

[3] G. Taylor, A. B. Rosenfeld, and B. J. Allen, "High resolution photon detection system for positron emission tomography," in *IPA PQ0853*, 2000.

[4] J. S. Huber, W. W. Moses, M. S. Andreaco, M. Loope, C. L. Melcher, and R. Nutt, "Geometry and surface treatment dependence of the light collection from LSO crystals," *Nucl. Instr. Meth.*, vol. A427, pp. 374–380, 1999.

[5] A. J. Bird, T. Carter, A. J. Dean, D. Ramsden, and B. M. Swinyard, "The optimization of small CsI(Tl) gamma-ray detectors," *IEEE Trans. Nucl. Sci.*, vol. 40, pp. 395–399, Aug. 1993.

[6] M. Moszynski, M. Kapusta, M. Mayhugh, D. Wolski, and S. O. Flyckt, "Absolute light output of scintillators," *IEEE Trans. Nucl. Sci.*, vol. 44, pp. 1052–1061, June 1997.